THE JOURNAL OF BIOLOGICAL CHEMISTRY
Vol. 278, No. 7, Issue of February 14, pp. 5333–5342, 2003
Printed in U.S.A.

Contribution of DNA Conformation and Topology in Right-handed DNA Wrapping by the *Bacillus subtilis* LrpC Protein*

Received for publication, July 25, 2002, and in revised form, November 18, 2002
Published, JBC Papers in Press, November 27, 2002, DOI 10.1074/jbc.M207489200

Christophe Beloin‡§¶, Josette Jeusset‖, Bernard Révet‖, Gilles Mirambeau‖, Françoise Le Hégarat‡, and Eric Le Cam‖**

From the ‡Institut de Génétique et Microbiologie, Université Paris XI, Unité Mixte Recherche 8621, Bâtiment 360, 91405 Orsay Cedex, France, and ‖Laboratoire de Microscopie Cellulaire et Moléculaire, Institut Gustave Roussy, Unité Mixte Recherche 8126, 94805 Villejuif Cedex, France

The *Bacillus subtilis* LrpC protein belongs to the Lrp/AsnC family of transcriptional regulators. It binds the upstream region of the *lrpC* gene and autoregulates its expression. In this study, we have dissected the mechanisms that govern the interaction of LrpC with DNA by electrophoretic mobility shift assay, electron microscopy, and atomic force microscopy. LrpC is a structure-specific DNA binding protein that forms stable complexes with curved sequences containing phased A tracts and wraps DNA to form spherical, nucleosome-like structures. Formation of such wraps, initiated by cooperative binding of LrpC to DNA, results from optimal protein/protein interactions specified by the DNA conformation. In addition, we have demonstrated that LrpC constrains positive supercoils by wrapping the DNA in a right-handed superhelix, as visualized by electron microscopy.

The structural properties of DNA and specific DNA/protein interactions are crucial for the regulation of fundamental cellular processes such as recombination, replication, and chromosome organization. In prokaryotes, several small DNA binding proteins regulate these processes by local changes in DNA conformation, through the formation of specific nucleoprotein complexes. In *Escherichia coli*, these small DNA binding proteins include the CRP, IHF, Fis, H-NS, Dps, Lrp, and HU proteins (1), and in *Bacillus subtilis*, the HU-like protein, HBsu (2). Notably, these proteins can regulate DNA transcription. For example, CRP, IHF, and Fis facilitate the association of RNA polymerase with upstream DNA sequences or with activator proteins, and can enhance the interactions of activator or repressor proteins at distant sites (3, 4). Moreover, HU binding to promoter regions modulates the binding of other transcriptional regulators like CRP (5), LexA (6) and GalR (7). Change of DNA conformation by protein/DNA interaction, however, is not limited to prokaryotic species. Numerous eukaryotic proteins (*e.g.* transcription factors, such as TBP or TFIIIA, or structural high mobility group proteins, such as EF-1, SRY (8), HMG1 and HMG2 (9), and HMG-I(Y) (10)) use similar properties, particularly DNA bending, to regulate transcription.

The *lrpC* gene was identified during the *B. subtilis* genome-sequencing project (11). It encodes a neutral 16.4-kDa protein, LrpC, that forms tetramers in solution. Based on amino acid sequence identity, it has been assigned to the Lrp/AsnC family of transcriptional regulators, which in *B. subtilis* includes seven Lrp/AsnC-like proteins (12–14). The N-terminal region of LrpC is predicted to form a typical helix-turn-helix DNA binding domain, characteristic of numerous transcriptional regulators (15). Previous experiments have shown that the *lrpC* gene is autoregulated (16). In addition, phenotypic analysis of a *lrpC* mutant in *B. subtilis* has revealed a possible role of LrpC in branched chain amino-acid metabolism, sporulation, and long-term adaptation to stress (16).

To analyze in detail the interactions of LrpC with DNA, the experiments presented here combine electrophoretic mobility shift assays (EMSA),[1] electron microscopy (EM), and atomic force microscopy (AFM), using the *lrpC* promoter DNA, and curved DNA fragments. These studies show that LrpC possesses unusual DNA architectural properties not previously assigned to Lrp-like proteins or other general DNA-structuring proteins and that DNA curvature and DNA topology (*i.e.* supra-architecture) control the order of events in protein/DNA complex formation.

EXPERIMENTAL PROCEDURES

DNAs and Protein—The 648-bp fragment encompassing the *lrpC* promoter region was obtained by a *Pvu*II digestion of the plasmid pUC18*prolrpC* (16). Shorter, 331-bp DNA fragments containing 5′-*lrpC* region used in EM and AFM experiments were obtained by PCR and purified by an anion exchange MonoQ column using a SMART system (Amersham Biosciences); α and β fragments correspond, respectively, to -225 to $+106$ and -270 to $+61$ with respect to the *P1* transcription start site.

The β fragment was biotinylated at its 5′- or 3′-extremity and dimerized using streptavidin. After dimerization of the β fragment the promoters *P1/P2* are localized near the extremities when using the 5′-biotinylated fragment (5′β-dimers) or near the center using the 3′-biotinylated fragment (3′β-dimers).

The DNA fragments containing the different curved regions of pBR322 were obtained by PCR amplification (pC4–6, 1773 bp, position 1185–2958; pC7, 1444 bp, position 2576–4020; and pC8, 722 bp, position 3946–307). The 1444-bp fragment containing C7 curved region was end-labeled at its 3′ extremity using a biotinylated primer. The labeling was revealed by the streptavidin ferritin system (17). Curvature of the pBR322 was determined using the DNA ReSCue program (17, 18).

Plasmid pBR322 was used in both EMSA and EM experiments.

* This work was supported in part by grants from CNRS/Université Paris XI (UMR C8621 and ARC 9490 to F. L. H. and CNRS UMR 8126 to E. L. C.). The costs of publication of this article were defrayed in part by the payment of page charges. This article must therefore be hereby marked "*advertisement*" in accordance with 18 U.S.C. Section 1734 solely to indicate this fact.

§ Present address: Groupe de Génétique des Biofilms, Bâtiment Fernbach, Institut Pasteur, 25 rue du Dr Roux, 75724 Paris cedex 15, France.

¶ Supported by fellowships from the French Ministère de l'Éducation Nationale, de l'Enseignement Supérieur et de la Recherche, and Fondation pour la Recherche Médicale.

** To whom correspondence should be addressed. Tel.: 33-1-69-15-63-62; Fax: 33-1-69-15-63-34; E-mail: francoise.le-hegarat@igmors.u-psud.fr.

[1] The abbreviations used are: EMSA, electrophoretic mobility shift assay; EM, electron microscopy; AFM, atomic force microscopy.

Supercoiled pBR322 was from Amersham Biosciences and linear pBR322 DNA was obtained by a *Sal*I digestion of the plasmid. It was then purified using the High Pure PCR product purification kit from Roche Molecular Biochemicals. Relaxed DNA used in relaxation assays was from Lucent Ltd. Topoisomers of plasmid pTZ18R were prepared by a topoisomerase I assay in presence of ethidium bromide to obtain negative topoisomers and in presence of netropsin to obtain positive topoisomers.

The LrpC protein was previously purified (16) and shown to form tetramers in solution (data not shown; 19). Consequently, all the concentrations of protein used in this work correspond to LrpC tetramers.

Protein/DNA Binding—A typical EMSA mixture contained 25 mM Tris-HCl, pH 8, 50 mM NaCl, 10% glycerol, 0.1 mM EDTA, 5 mM $MgCl_2$, 1 mM dithiothreitol, 0.1 mM phenylmethylsulfonyl fluoride (binding buffer M) with or without 4 mM spermidine, ~0.5 nM ^{32}P-end-labeled DNA probe, and purified LrpC protein in a volume of 20 μl. For plasmid DNA, unlabeled pBR322 plasmid (2 nM) and binding buffer M without spermidine were used. After incubation for 10 min at room temperature, the reaction was loaded onto a 6% acrylamide/*N*,*N*′-methylenebisacrylamide (final ratio, 80:1) gel containing 10% glycerol or onto a 0.7% agarose gel in 44.5 mM Tris borate, 2 mM EDTA, pH 8.3 (0.5× Tris borate/EDTA). Electrophoresis was performed at 10 V/cm and at 4 °C. Radioactive gels were dried, visualized by autoradiography, and sometimes quantified with a PhosphorImager (Amersham Biosciences). Nonradioactive gels were stained in 0.5× Tris borate/EDTA containing 0.2 μg/ml ethidium bromide.

Observation of LrpC/DNA Complexes by Electron Microscopy and Atomic Force Microscopy—Complexes were formed as described for EMSA with the following modifications. Dithiothreitol, phenylmethylsulfonyl fluoride, and spermidine were removed from binding buffer M to avoid any interference or artifact that might be caused by these components. The volume of the assay mixture was 40 μl. After incubation for 10 min at room temperature, the complexes were purified by gel filtration (Superose 6B; Amersham Biosciences), with a SMART system to remove unbound protein and to reduce nonspecific binding. EM observations were performed as described previously (20). 5 μl of LrpC/DNA complexes, at a concentration of 0.5 μg/ml of DNA, were deposited onto a 600 mesh copper grid covered with a thin carbon film activated by a glow discharge in the presence of pentylamine (21). Grids were washed with aqueous 2% uranyl acetate, dried, and observed in annular darkfield in a Zeiss 902 electron microscope. Using this spreading procedure, DNA molecules are rapidly adsorbed onto the carbon film with no major loss in the tridimensional information (22). LrpC-DNA complexes were observed at a final magnification of 340,000× on a TV screen. Images of LrpC-bound DNA molecules were stored and digitized with a Kontron image processing system as described previously (17). The data were processed in a PC computer and the DNA-protein interactions were mapped from 250 complexes. DNA foreshortening gives an estimation of the length wrapped around the particle.

To analyze LrpC/DNA complexes by AFM, 20 μl of the same solutions used for EM in presence of 5 mM Mg^{2+} were deposited onto freshly cleaved mica and then washed with 0.2% (w/v) aqueous uranyl acetate (23). The observation was performed in the tapping mode in air specifically available with nanoscope IIIa (Digital Instruments/Veeco).

Effect of LrpC on DNA Supercoiling in Vitro—Different amounts of LrpC, ranging from 37.5 to 1500 nM (in tetramers), were incubated with 20 nM of pBR322 (supercoiled or relaxed) at room temperature for 15 min in a total volume of 10 μl of buffer containing 20 mM Tris-HCl, pH 7.5, 50 mM NaCl, 0.1 mM EDTA, 1 mM DTT, and 20% glycerol. Wheat germ topoisomerase I (2 unit) was then added and the incubation continued for 150 min at 37 °C. The DNA was deproteinized by adding SDS and NaCl to a final concentration of 1% and 1.7 M respectively, followed by extraction with phenol/chloroform/isoamyl alcohol (25/24/1 v/v) and the DNA precipitated with 100% ethanol. The DNA pellet was resuspended in 10 μl of buffer containing 10 mM Tris-HCl, pH 7.5, 1 mM EDTA and loaded onto a 1% agarose gel. One-dimensional electrophoresis was performed for 16 h at 1.5 V/cm in Tris acetate/EDTA buffer (40 mM Tris-HCl, pH 8.3, 25 mM sodium acetate, and 1 mM EDTA). Two-dimensional electrophoresis was performed as follows: in the first dimension, samples were separated in 1% agarose for 6 h at 3 V/cm in Tris acetate/EDTA buffer. The gel was then equilibrated for 30 min in Tris acetate/EDTA buffer containing 10 ng/ml ethidium bromide. The second dimension of electrophoresis was performed for 16 h at 1.3 V/cm in the same buffer. Gels were stained with 0.2 μg/ml ethidium bromide.

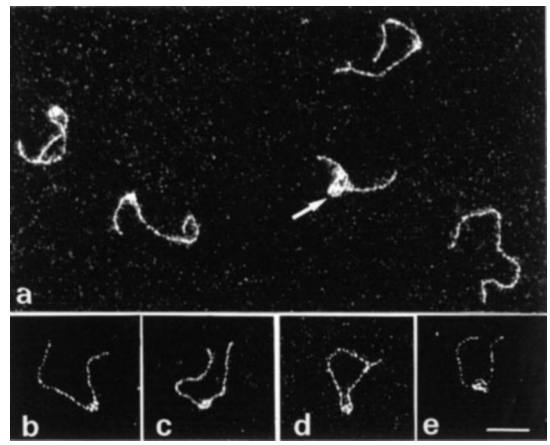

FIG. 1. **Visualization of LrpC binding to the *lrpC* promoter region.** A 648-bp fragment (1 nM) containing 331 bp of the 5′-*lrpC* region (−225 to +106 with respect to *P1*) and flanked by 120 and 197 bp of pUC18 plasmid DNA was mixed with purified LrpC at a protein/DNA molar ratio of 6:1 (one tetramer/100 bp). LrpC/DNA complexes were visualized by EM. *a*, different types of protein/DNA complexes that formed compared with uncomplexed DNA (molecule at *bottom right*). The presence of the protein correlates with thickening of some parts of the DNA. The LrpC/DNA complex indicated by an *arrow* shows highly condensed DNA caused by successive wrappings. *b–e*, representative LrpC/DNA complexes indicating the different steps in the wrapping mechanism. In *e*, a tight wrapping of more than one superhelical turn of DNA is shown. *Scale bar*, 50 nm.

RESULTS

The effect of LrpC on lrpC Promoter Architecture—Previous experiments have shown that the LrpC protein binds the upstream region of the *lrpC* gene *in vitro* (16, 19). As many transcriptional regulators are known to modify the geometry of their target promoters, we wanted to determine whether LrpC displays such a property. Therefore, the interaction of LrpC with the *lrpC* promoter region was visualized by EM. Purified LrpC protein was incubated with a 648-bp DNA fragment digested from plasmid pUC18prolrpC that contains the α fragment in Fig. 2*A*, this is 331-bp of the 5′-*lrpC* region (16). Protein/DNA complexes were visualized by EM using an annular darkfield mode (24).

The simultaneous presence of free DNA molecules and of LrpC/DNA complexes, which were either partially or completely condensed (Fig. 1*a*) confirms the cooperative binding of LrpC to DNA as shown previously (16). Some DNA molecules displayed thickening that was sometimes associated with bending of the DNA (Fig. 1; data not shown). Various degrees of organization of the *lrpC* promoter were observed, ranging from a local binding of LrpC along the DNA to DNA wrapping (Fig. 1, *b–e*). It is tempting to suggest that these series of micrographs, as displayed in the order *b* to *e* actually represent the progressive interaction of LrpC with DNA. Measurements of DNA length in LrpC/DNA complexes indicated that such interaction corresponds either to less than one turn of the DNA molecule around the protein core (Fig. 1, *c* and *d*) or to the wrapping of more than one turn of the DNA (Fig. 1, *a*, *arrow*, and *e*), which thus seems shorter.

LrpC Wraps DNA to Form Nucleosome-like Structures—The conformation of the 648-bp DNA fragment containing the *lrpC* promoter was significantly altered when bound by the LrpC protein. To further investigate this change in DNA conformation, we analyzed the interactions of LrpC with the α fragment itself, which encompasses only the 5′-*lrpC* region (Fig. 2*A*, α fragment, −225 to +106 with respect to the *P1* transcription start site). Protein/DNA complexes were allowed to form for different lengths of time using a LrpC/DNA molar ratio of 4:1 (LrpC protein concentration in tetramers, its preferred quater-

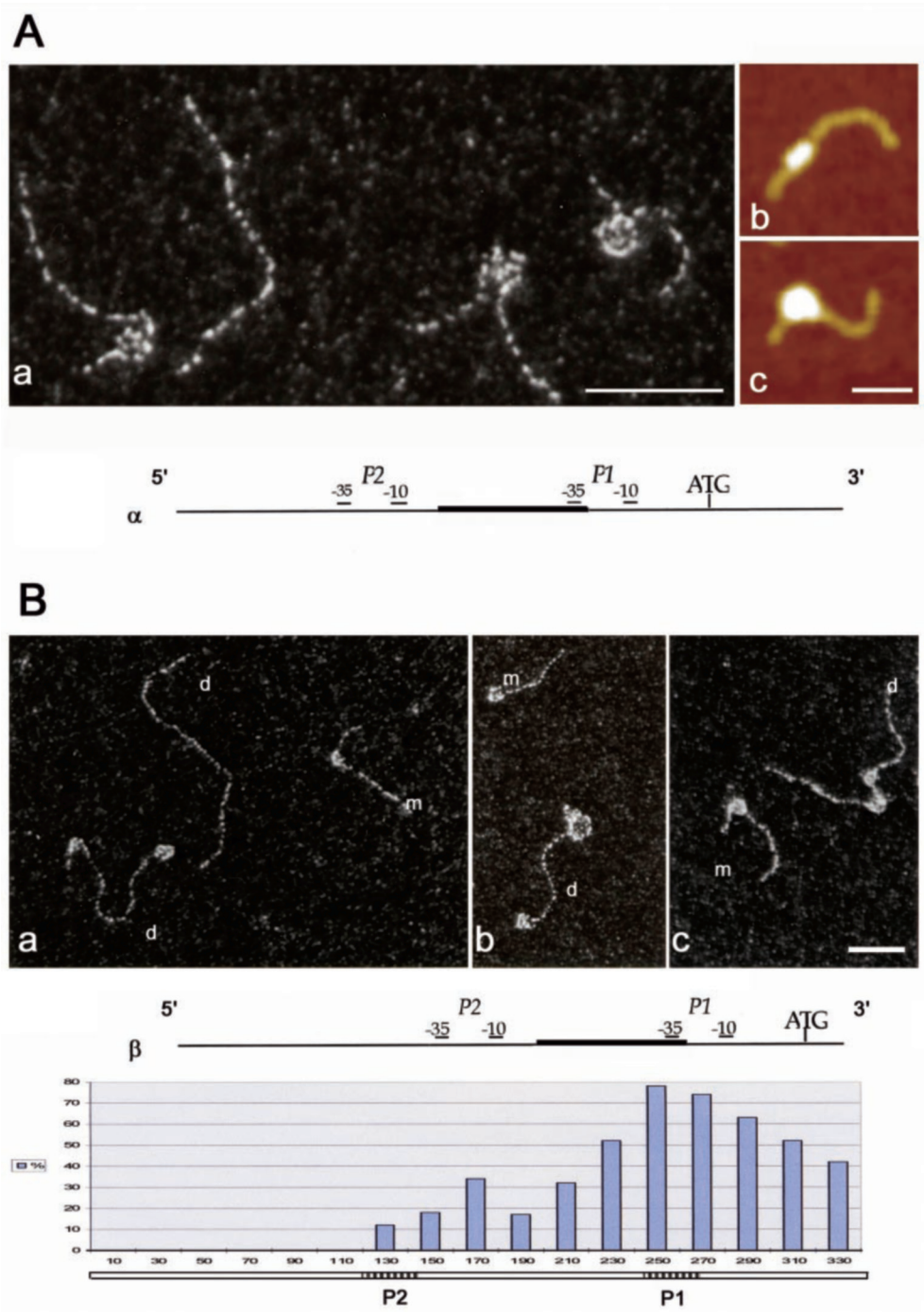

FIG. 2. **Structure and mapping of the LrpC/DNA complex.** *A*, EM and AFM visualization of LrpC/DNA nucleosome-like complexes. Purified LrpC was incubated with the DNA α fragment (−225 to +106 with respect to the *lrpC P1*promoter) and the wrapping of DNA around LrpC was analyzed by EM (*a*) (140,000×). *b* and *c*, representative LrpC/α DNA fragment visualized by AFM without (*b*) or with (*c*) DNA wrapping. *B*, mapping the LrpC binding site within the *lrpC* promoter region. The β fragment (−270 to +61 with respect to *P1*) was biotinylated at its 5′- or 3′-extremity and dimerized using streptavidin (5′β- and 3′β-dimers, respectively). Promoters *P1*/*P2* are localized near the extremities of 5′β-dimers (*a* and *b*) or near the center of 3′β-dimers (*c*). Monomers of β fragments are also present in the preparation and are complexed at their extremities by LrpC. The precise LrpC binding sites of 250 LrpC/5′β dimers complexes were mapped, and the data presented in the histogram show the total percentage of interactions within 20-bp windows. *m* and *d* represent monomers and dimers of β fragments, respectively. *A* and *B*, *scale bars*, 50 nm. The α and β fragments used above are represented with the wedge-curved sequence (*black box*) localized between *P2* and *P1* −35 box, whereas the junction-curved DNA is localized between *P1* −35 box and the *lrpC* ATG.

nary structure in solution). The complexes were subsequently visualized by EM at high magnification (140,000×). After 1–10 min, the complexes seemed to be localized at various positions of the α fragment, although a preference at or near the extremities was observed (data not shown). After a longer incubation time (15 min), LrpC seemed to be nearer to the center of the α fragment, with the DNA molecule clearly tightly wrapped around it (Fig. 2*A*). This LrpC-mediated DNA wrapping creates spherical structures resembling nucleosomes (Fig. 2*A*, *a*). The contour length of the DNA wrapped around LrpC (averaged from measuring 50 LrpC/DNA complexes; see "Experimental Procedures") was 28 ± 4 nm, which corresponds to 80 ± 12 bp, and the radius of curvature was 4.5 ± 0.2 nm. The presence of intrinsic curvature in the *lrpC* promoter region presumably

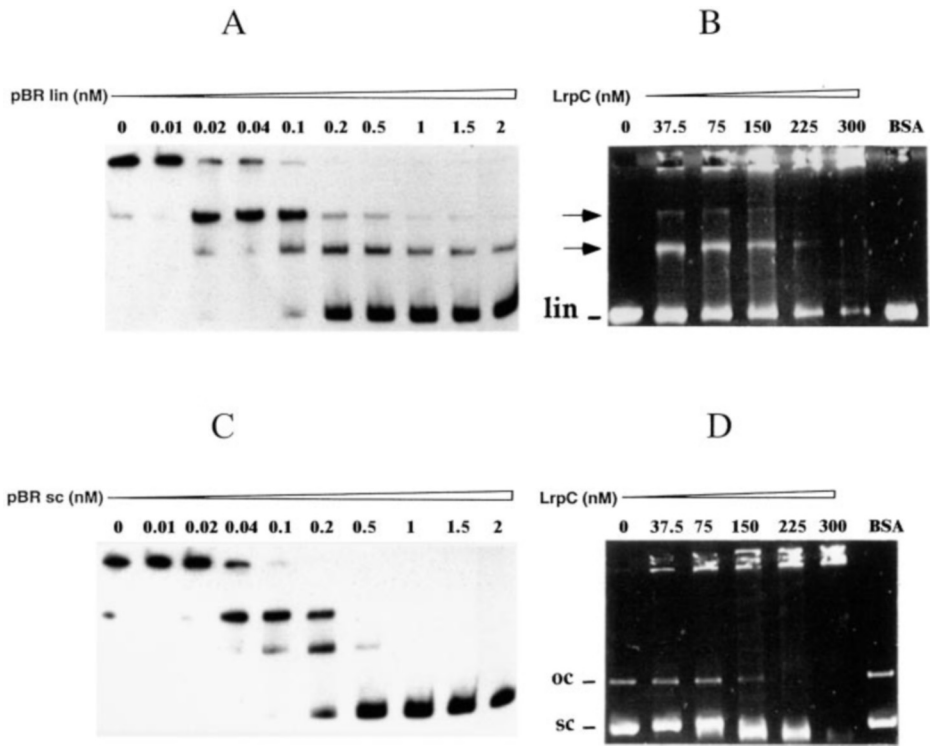

FIG. 3. **LrpC binding has different effects on linear and on supercoiled plasmid DNA.** In competitive EMSA, ^{32}P-labeled 5′-*lrpC* β fragment (0.5 nM) was incubated with an excess of purified LrpC (12 nM) and increasing amounts (0 to 2 nM) of unlabeled linear pBR322 (pBRlin, *A*) or supercoiled pBR322 (pBRsc, *C*) as competitor DNA. Complexes were resolved by migration through a 6% polyacrylamide gel. In direct plasmid EMSA, 2 nM of linear pBR322 DNA (*B*) or negatively supercoiled pBR322 DNA (*D*) was incubated with an increasing concentration of LrpC (0 to 300 nM). Complexes were resolved by migration through a 0.7% agarose gel. Protein/DNA complexes were visualized by staining with ethidium bromide. 400 ng of bovine serum albumin (*BSA*) was incubated with the plasmids as a negative control. Linear plasmid (*lin*) corresponds to *Sal*I-digested supercoiled pBR322 (*sc*). LrpC/lin complexes are indicated by *arrows*. Purified supercoiled pBR322 contains traces of open circular plasmid as indicated (*oc*).

promotes the DNA wrapping around LrpC (16). As shown in Fig. 1, several LrpC/DNA complexes resulted from multiple wrappings of the DNA that induced a highly ordered condensation (data not shown).

We also used AFM under air-dried conditions to obtain topographic information about the LrpC/DNA complexes. The main results shown in Fig. 2*A*, *b*, confirmed that the thickenings observed by EM (Figs. 1 and 7) were really caused by the presence of the protein. LrpC covered various lengths of DNA, but such complexes were not always associated with DNA bending. LrpC binding therefore seems to progress until stable wrappings are formed (Fig. 2*A*, *a*) resulting also in spherical structures.

Localization of the LrpC Binding Site on the lrpC Promoter—To map the location of LrpC binding to the *lrpC* promoter DNA fragment, we have used the β fragment (Fig. 2*B*, −270 to +61 with respect to the *P1* transcription start site). The β fragment has the same length as the α fragment, but the *P1* promoter region is much closer to the extremity of the DNA molecule. To distinguish the extremity of the fragment that contains the P1 promoter, β fragments were bridged by their 5′ (5′β dimers) or 3′ (3′β dimers) extremities (see "Experimental Procedures"). In the 5′β dimers, the *P1* promoter regions localized at the extremities of the dimers. In the 3′β dimers, the *P1* promoter regions are gathered at the center of the dimers. When LrpC was incubated with either the 5′β dimers (Fig. 2*B*, *a* and *b*) or the 3′β dimers (Fig. 2*B*, *c*), its binding coincided with the position of the *P1* promoter as visualized by EM. Some unbridged β monomers present in the preparation were complexed with LrpC at their extremities. 250 LrpC/5′β complexes were mapped to the precise location of LrpC. 78% of the LrpC/5′β dimer complexes had LrpC bound at the *P1* promoter region. Only 10–20% of the complexes had LrpC localized at the *P2* promoter region. The average length of DNA complexed with LrpC was 90 bp with an S.D. of 42.5 bp. Multiple DNA wrappings around LrpC were also observed here (data not shown).

Binding of LrpC to Linear versus Supercoiled Plasmid DNA—LrpC DNA binding properties described above are not restricted to the *lrpC* promoter region. This was first demonstrated in an EMSA by using pBR322 DNA as a competitor for the previously shown binding of LrpC to a ^{32}P-labeled *lrpC* promoter DNA fragment (Fig. 3, *A* and *C*) (16). Increasing concentrations of plasmid DNA were able to disrupt the highly retarded radioactive complex LrpC/*lrpC* promoter (Fig. 3, *A* and *C*). Moreover, a remarkable difference was observed in the competing ability of the linear and of the supercoiled pBR322 monitored by EMSA. Up to 0.2 nM the linear form is more able than the supercoiled form to compete with the labeled *lrpC* promoter region for the LrpC protein. Consequently, a larger fraction of the LrpC bound DNA is released from the LrpC protein and can move further in the electric field (Fig. 3*A*). At higher pBR322 concentrations, the supercoiled form is more effective to bind the LrpC protein and the totality of the labeled DNA is even free from the LrpC protein (Fig. 3*C*).

The binding between LrpC and pBR322 DNA was also confirmed directly (Fig. 3, *B* and *D*). At low LrpC concentrations, a small proportion of linear pBR322 was shifted and led to clearly defined retarded complexes (Fig. 3*B*, *arrows*) whereas at higher concentrations of LrpC, the totality of the DNA remained in the wells. Curiously, the binding of LrpC to supercoiled pBR322 was somewhat different (Fig. 3*D*). Whereas linear pBR322 caused gel retardation as expected on the basis of the competition experiment, the supercoiled pBR322 showed

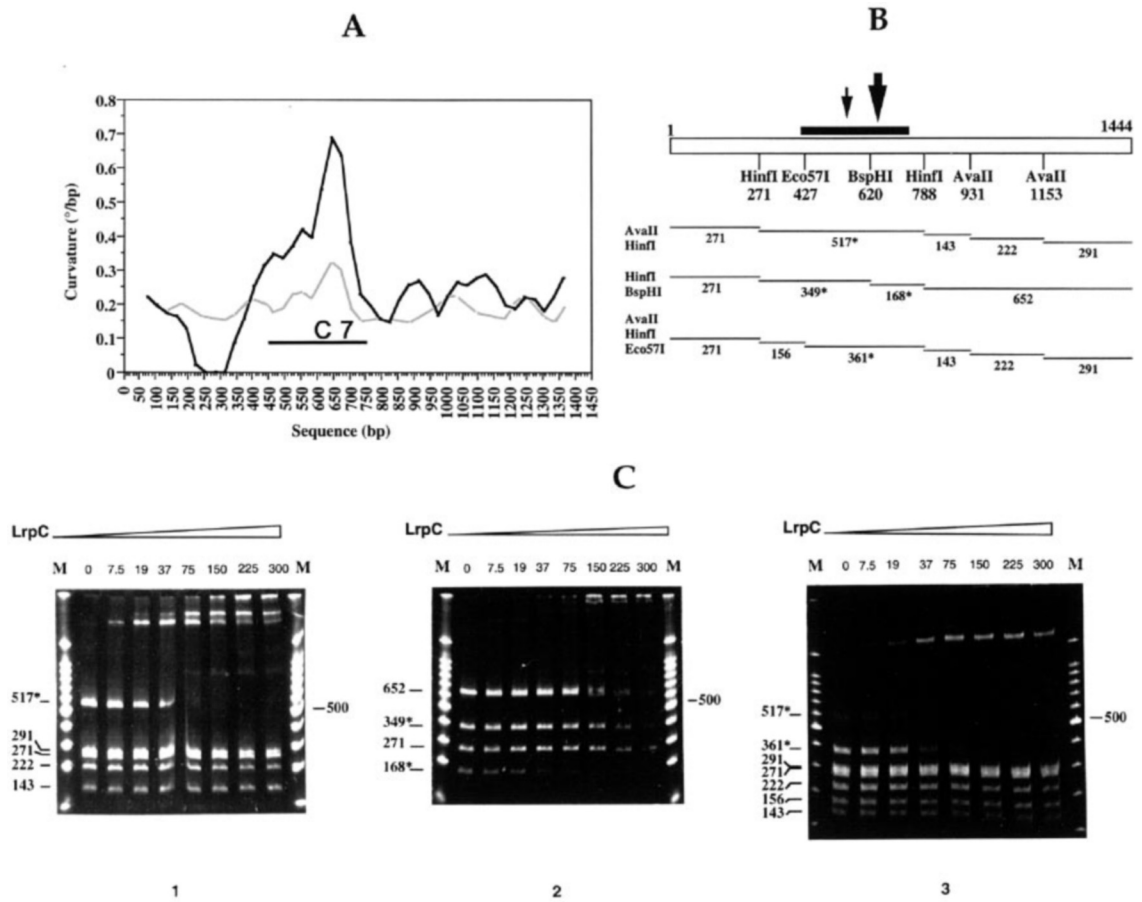

FIG. 4. **Identification of a curved region of pBR322 to which LrpC preferentially binds.** *A*, analysis of DNA curvature. A 1444-bp *Taq*I-*Taq*I fragment of pBR322 (position 2576 to 4020) that is preferentially bound by LrpC was subjected to curvature detection analysis using the DNA ReSCue program (18). The propensity plots indicating curvature (degree per base pair) according to Refs. 45 (*gray line*) and 46 (*black line*), plotted against the position in the sequence, are presented. The DNA corresponding to the C7 curved region is indicated (410 to 750 bp in the 1444-bp *Taq*I-*Taq*I fragment that corresponds to 2986 to 3301 bp in pBR322). The C7 DNA contains two curved regions, the first only slightly curved and located between 410 and 600 bp with a maximum curvature at 550 bp and a second one extended from 600 to 750 bp with a maximum curvature at 650 bp. *B*, schematic representation of the 1444-bp fragment with the C7 curved region (*thick line*). The maximum of the major curvature (650 bp) is indicated by the *thick arrow*, whereas the maximum of the minor curvature (550 bp) is indicated by the *thin arrow*. The positions of relevant restriction endonuclease cleavage sites are shown. Three sets of DNA fragments encompassing different regions of the 1444-bp fragment were generated by using different enzyme combinations. *, restriction fragments that include a part of or the entire C7 curved region. *C*, EMSA of LrpC interactions with restricted segments of the 1444-bp *Taq*I-*Taq*I fragment of pBR322. The 1444-bp *Taq*I-*Taq*I fragment (10 nM) was digested with *Ava*II-*Hinf*I (*1*), *Hinf*I-*Bsp*HI (*2*), or *Ava*II-*Hinf*I-*Eco*57I (*3*) and incubated with increasing concentrations of LrpC (0 to 300 nM). Complexes were resolved through a 6% acrylamide gel in 0.5× Tris borate/EDTA at 4 °C. *M*, Promega 100-bp DNA ladder. *, restriction fragments that include a part of or the entire C7 curved region.

very weak retardation of the totality of the DNA at LrpC concentrations of 37.5 and 75 nM (Fig. 3*D*). At higher concentrations of LrpC (150 and 225 nM), the protein even slightly increased the mobility of most of the supercoiled DNA. At 300 nM LrpC, a large proportion of the DNA was stuck in the wells. In comparison, the open circular form of plasmid pBR322 was not bound at LrpC concentrations below 150 nM, suggesting a lower affinity of LrpC for open circular DNA. Altogether, these results show that LrpC interacts quite differently with the various topological forms of the same DNA molecule.

Selective Recognition of LrpC within the Different Curved Regions of pBR322—LrpC shows selectivity in forming complexes with linear pBR322 DNA. The presence of preferential LrpC binding sites was investigated by EMSA. The 1444-bp *Taq*I-*Taq*I restriction fragment (see Fig. 5*B* for details) was preferentially bound by LrpC (data not shown). It contains a curved region described previously as C7 (Fig. 4*A*; Ref. 17). To identify more precisely the region(s) recognized by LrpC within this fragment, it was cleaved by restriction enzymes into three different sets of DNA fragments (Fig. 4*B*). Interestingly, a 517-bp fragment that encompasses the C7 curved sequence was preferentially bound by LrpC (Fig. 4*C*, *1*). When the curvature or its position within the fragment was altered, the preferential binding was lost (Fig. 4*C*, *2*; the 517-bp fragment is cut into 349- and 168-bp fragments). Finally, a 361-bp fragment containing only the C7 region was specifically bound by LrpC (Fig. 4*C*, *3*). A precise localization of the LrpC binding site was performed using a 1444-bp biotinylated fragment and EM observation (see "Experimental Procedures"; Fig. 5*A*, *c* and *d*). The complexes were visualized between positions 490 and 720, covering about 80 bp (± 20 bp) (data not shown). This corresponds exactly to the position of the curved region detected in C7 (Fig. 4*A*).

Because pBR322 contains three other major curved regions (*i.e.* C4, C6, and C8 (17)) (Fig. 5*B*), we sought to investigate the differential affinity of LrpC for these curved regions. To this effect, three DNA fragments were amplified from pBR322 by PCR. These contained the C4-C6 region (pc4–6), the C7 region (pc7), and the C8 region (pc8). The three fragments were mixed at equimolar concentration, incubated at an LrpC/DNA molar ratio of 12.5, and 200 complexes were analyzed by EM (Fig. 5*A*, *a*). No LrpC/pc4–6 complexes were observed, whereas 44% of

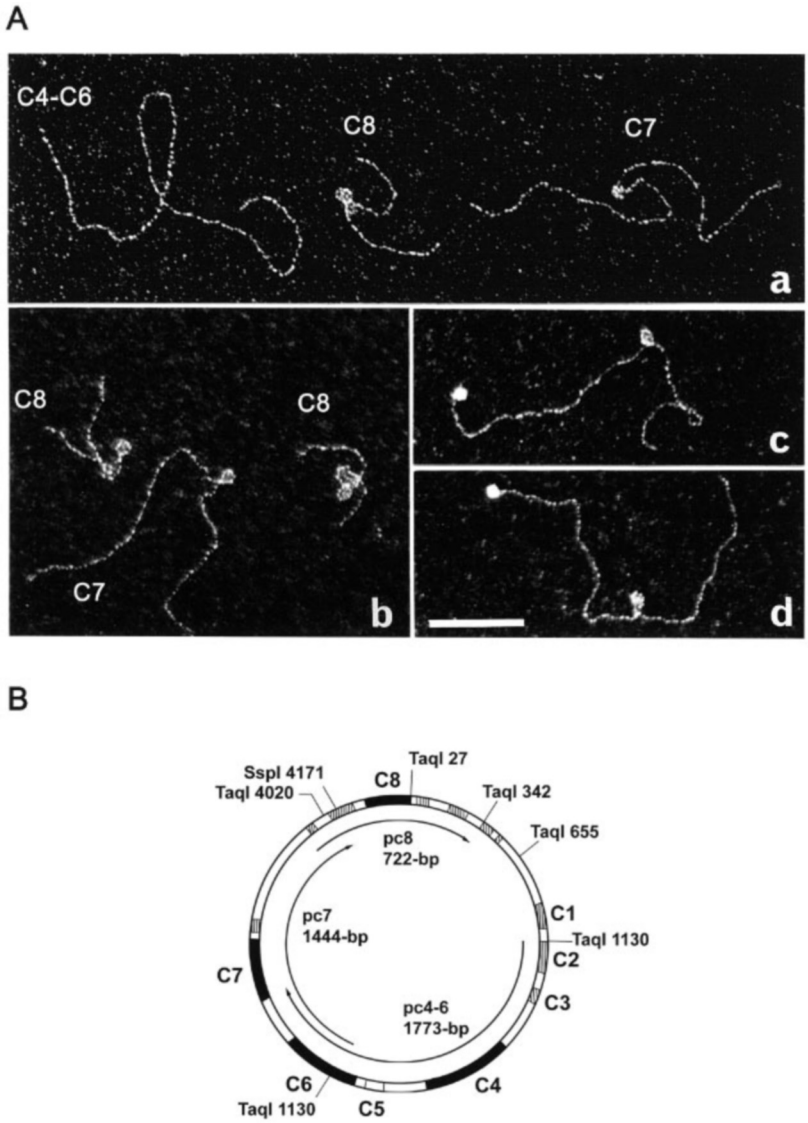

FIG. 5. **LrpC binds preferentially to the C7 and C8 regions of pBR322.** *A*, EM visualization of LrpC association with curved DNA. Three PCR fragments were generated that contain the C4-C6 (1773 bp, pc4–6), C7 (1444 bp, pc7), and C8 (722 bp, pc8) pBR322 curved regions. These fragments (5 nM) were co-incubated with 100 nM of LrpC. Complexes formed were observed by EM (*a* and *b*). To localize the binding of LrpC to the C7 curved region, the pc7 fragment was labeled by biotin-streptavidin-ferritin at its 3′-extremity and complexes formed with LrpC were visualized by EM (*c* and *d*). The bar represents 100 nm. *B*, schematic representation of the curved regions of pBR322. This diagram is adapted from Ref. 17. Minor curved regions including C1, C2, C3, and C5 are *hatched*. Major curved regions C4, C6, C7, and C8 are indicated by *black boxes*. PCR fragments containing C4-C6, C7, or C8 regions are represented by *arrows*.

the pc8 fragments were complexed with LrpC. Consistent with the results presented above, 78% of the pc7 fragments were found to be associated with LrpC. LrpC binding to the C7 and C8 regions led to the formation of stable wraps/loops as observed with the *lrpC* promoter region (Fig. 5*A*, *a–d*). Therefore, the presence of curvature favored the wrapping of DNA around LrpC. Interestingly, the sequence analysis of pc8 revealed that it has two series of oligoA tracts in phase (*i.e.* on the same side of the DNA double helix) that create two successive, sharply curved domains that could be potential targets for LrpC. Indeed, double wrappings were frequently observed within LrpC/pc8 complexes, as is clearly visible in Fig. 5*A*, *b*.

LrpC Positively Supercoils DNA—After showing the influence of DNA curvature on the formation of the LrpC/DNA complexes, we investigated the effect of LrpC on DNA topology. Increasing amounts of purified LrpC protein were incubated with relaxed closed circular pBR322 DNA. Subsequently, wheat germ topoisomerase I was added to relax any formation of compensatory supercoils elsewhere in the free DNA. The pBR322 DNA was deproteinized and analyzed by agarose gel electrophoresis to resolve topoisomers (Fig. 6*A*). Incubation of pBR322 DNA with increasing concentrations of LrpC in combination with the action of the topoisomerase I resulted in extended supercoiling and generated a large distribution of distinct topoisomers. Indeed, at a LrpC/DNA molar ratio of 75:1 (one tetramer of LrpC per 60 bp), 11 topoisomers could be resolved (Fig. 6*A*, *lane b*). These experiments clearly demonstrate that LrpC interaction with pBR322 in presence of topoisomerase I introduces supercoils into a closed circular DNA, consistent with Ref. 19.

To ascertain whether the supercoils constrained by LrpC were negative or positive, pBR322 samples that were incubated without LrpC (Fig. 6*A*, *a*) or with 1500 nM LrpC (Fig. 6*A*, *b*) were separated by two-dimensional agarose gel electrophoresis (Fig. 6*B*). A mixture of negatively and positively supercoiled topoisomers migrates as a biphasic arched pattern of bands. In the presence of LrpC, the arch of topoisomers corresponded exclusively to positively supercoiled topoisomers (Fig. 6*B, b*), whereas, without LrpC, the distribution of DNA topoisomers corresponded to the relaxed state (Fig. 6*B*, *a*). Therefore, it can be concluded that most of the DNA bound to LrpC protein is positively supercoiled.

LrpC Wraps DNA in a Right-handed Superhelix—We have shown that LrpC binds to negatively supercoiled pBR322 DNA (Fig. 3*B*); however, LrpC constrains positive supercoils in closed circular DNA (Fig. 6). Therefore, binding of LrpC to different forms of pBR322 plasmid DNA was further analyzed by EM. LrpC was incubated with an equimolar concentration of linear and supercoiled plasmid DNA at a LrpC/DNA ratio of 37/1 (corresponding to one LrpC tetramer per 118 bp). Only 5%

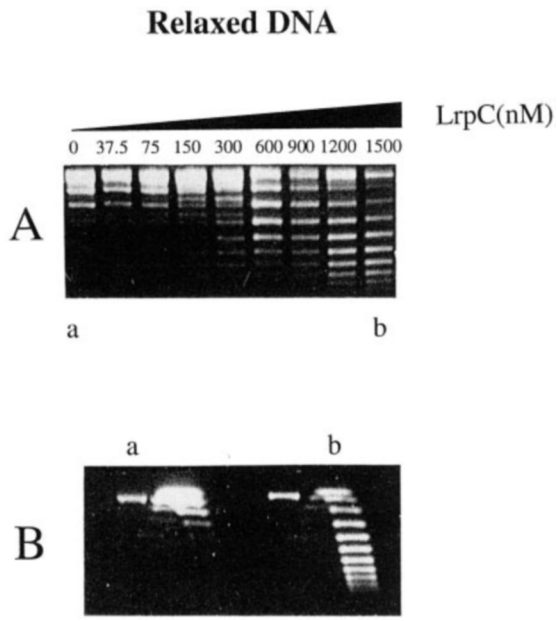

FIG. 6. **LrpC constrains positive supercoils in relaxed pBR322.** Topoisomerase I relaxation assay. *A*, relaxed pBR322 (20 nM) was incubated with increasing amounts of LrpC (37.5 to 1500 nM) for 15 min at room temperature. TopoI was then added and incubation continued for 150 min at 37 °C. Deproteinized samples were separated on a one-dimensional agarose gel. *B*, pBR322 DNA without LrpC (*a*), and with 1500 nm LrpC (*b*), as indicated, were separated by two-dimensional agarose gel electrophoresis with ethidium bromide in the second dimension. The positive topoisomers constrained by LrpC are clearly visible in sample *b*.

of the open form of the plasmid (linear and traces of open circular DNA) were complexed with LrpC opposed to almost 100% for the supercoiled DNA. In the cases where LrpC associated with the linear or open circular plasmids, only one or two wrappings, appearing as small loops, were formed (Fig. 7*d*; data not shown). In contrast, the assembly of LrpC with negatively supercoiled DNA led to formation of five to six homogeneously structured loops (Fig. 7, *b–d*). This confirmed the selective affinity of LrpC for supercoiled DNA compared with linear DNA at high LrpC/DNA ratios. Moreover, these LrpC/DNA wrappings were frequently near each other in a restricted part of the molecule (Fig. 7*b*). The resulting topological constraints induced by loop formation seemed to be compensated by tight winding in other parts of the DNA, compared with free DNA molecules (compare Figs. 7*b* and 7*a*). Such a partition of DNA structural domains is clearly caused by an increase in the free negative supercoiling to compensate for the LrpC-restrained positive supercoils. This clearly demonstrates that the DNA is wrapped around LrpC as a right-handed superhelix, because left-handed wrapping of negatively supercoiled DNA would result in an apparent relaxation of the molecule. Furthermore, compared with free DNA (Fig. 7*a*), the part of the DNA exhibiting tight winding displayed thickening that could be caused by a local polymerization of LrpC on the DNA (Fig. 7, *b* and *c*). We also observed that within the same samples several supercoiled DNA molecules were highly compacted by the LrpC protein (Fig. 7*d*).

Considering the properties of LrpC, it was important to monitor its binding to positively supercoiled DNA. To this effect, we used a pBR322-derivative plasmid, pTZ18R, also

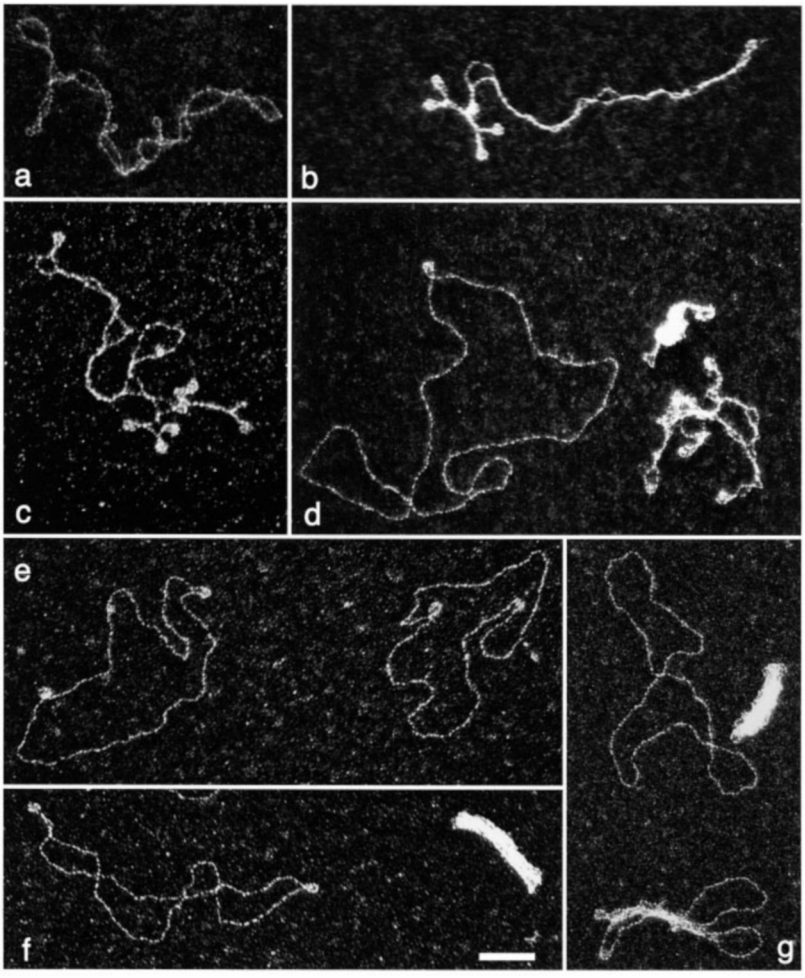

FIG. 7. **EM visualization of complexes between LrpC and supercoiled plasmid DNA.** *a*, a molecule of naked supercoiled pBR322. *b–d*, LrpC was incubated with an equimolar concentration of supercoiled pBR322 and linear plasmid DNA (protein/DNA molar ratio of 37:1 corresponding to one LrpC tetramer per 118 bp). A typical LrpC/supercoiled pBR322 complex conformation that was predominantly observed is shown in *b* and *c*. LrpC was rarely associated with linear DNA or open circular DNA molecules. However, a complex of LrpC with open circular pBR322 is shown on the left side of *d*. The ability of LrpC to highly condense supercoiled DNA is shown at the bottom right of *d–g*, corresponding to complexes of LrpC with positively supercoiled pTZ18R plasmid ($\Delta LZ = +4$) at a LrpC/DNA molar ratio of 8 (*e*) and 27 (*f* and *g*). *g*, *top left*, free pTZ18R DNA molecule. *Scale bar*, 50 nm.

containing the C7 and C8 regions. With the native negatively supercoiled form of pTZ18R ($\Delta L_k = -15$), we obtained the same pictures as with pBR322 (LrpC/DNA ratio of 28/1 corresponding to 1 LrpC tetramer per 100 bp, data not shown). However, when pTZ18R was artificially positively supercoiled ($\Delta L_k = +4$), only two loop complexes were observed (Fig. 7*e*, LrpC/DNA ratio of 8:1). Because positive supercoils are introduced by LrpC binding, the unbound DNA region is relaxed. When the LrpC/DNA ratio was increased to 27:1, a mixture of two types of complexes was observed: the two loops complexes already observed at a lower LrpC/DNA ratio and new complexes showing a very organized folding of the pTZ18R (+4) on itself (Fig. 7, *f* and *g*). As observed with native pBR322, LrpC was able to massively cover the DNA through cooperative mechanisms, thus promoting intramolecular condensation of DNA through LrpC/LrpC interactions.

DISCUSSION

We previously identified LrpC as the seventh member of the Lrp/AsnC family of proteins in *B. subtilis*, and we have shown that LrpC positively autoregulates its own gene. In this study, we have analyzed in detail the interactions of LrpC with DNA, with respect to DNA conformation, curvature, and topology, using EMSA, EM, and AFM. We showed that LrpC progresses unspecifically along DNA, preferentially recognizes a specific type of DNA curvature, and wraps DNA in a right-handed superhelix to form looped structures. In addition, we propose that its oligomerization on DNA is not random but is orientated by DNA conformation, mainly its bendability and its topological state. Moreover, LrpC is an unusual bacterial DNA architectural protein because of its capacity to constrain positive supercoiling. We propose a model for dynamic interactions between LrpC and DNA.

An Octameric Model for LrpC/DNA Interactions—We have provided evidence that LrpC wraps DNA and forms stable complexes resembling nucleosomes with various DNA fragments, including the *lrpC* promoter region, where its binding coincides with the *P1* promoter. Formation of stable complexes between LrpC and DNA results from protein-protein assembly. DNA flexibility or intrinsic curvature favors protein-protein interactions within one DNA fragment to form a stable protein core. This results in a progressive bending of the DNA that leads to loop formation through a complete wrapping of the DNA around the protein (Fig. 8*B*). LrpC could interact with DNA through its N-terminal helix-turn-helix motif and oligomerize through its C-terminal domain (Fig. 8*A*). The radius of curvature measured in the LrpC/DNA complexes correlates perfectly with the sizes of the octameric model presented for the recently crystallized LrpA protein of *Pyrococcus furiosus*, in which the four dimerized N-terminal DNA binding domains are diametrically opposed (25). Moreover, as with LrpA, LrpC has been shown to form dimers and multimers of dimers, mainly tetramers in solution (Ref. 19; data not shown).

DNA Conformation and Formation of Stable LrpC/DNA Complexes—DNA bendability determines the path of the double helix axis and contributes to the thermodynamic stabilization of the DNA/protein complexes. DNA bendability results from an increased local flexibility (26) and/or from a static intrinsic curvature, such as kinks or smooth continuous curvature, with either planar or torsional bending (27, 28). We demonstrated here that among different types of curvature, LrpC forms stable complexes with curved regions containing phased A tracts in pBR322 (C7 and C8; Fig. 5); in the *lrpC* promoter region (between the −35 box of *P1* and the ATG, Fig. 2*B*); and in synthetic curved DNA molecules (data not shown). These A tract motifs are related to the junction model, in which the deflection of the helix axis is localized at junctions between B′ form structure of A tracts and B form (29). Furthermore, all regions stably bound by LrpC contained phased A tracts preceded by a C (*i.e.* C(A)*n* motifs). In contrast, LrpC does not form any complexes with the pBR322 curved C4–C6 region (Fig. 5) or with the highly curved region located upstream of the −35 box of the *P1 lrpC* promoter (Fig. 2*B*; Ref. 16). In these fragments, curvature is more related to the wedge model, which attributes small deflections of the helix axis at every base-pair step, with a predominant contribution of the AA dinucleotide (30). Although junction and wedge models are comparable in their general predictions of DNA curvature for fragments, including phased A tracts, they differ for curved fragments without A tract motifs. Moreover, the wedge model does not take into account cooperativity effects in the stacking of AT base pairs within A tracts (31). Our results clearly show that LrpC discriminates between different types of curvature to form stable complexes within C(A)*n* phased motifs.

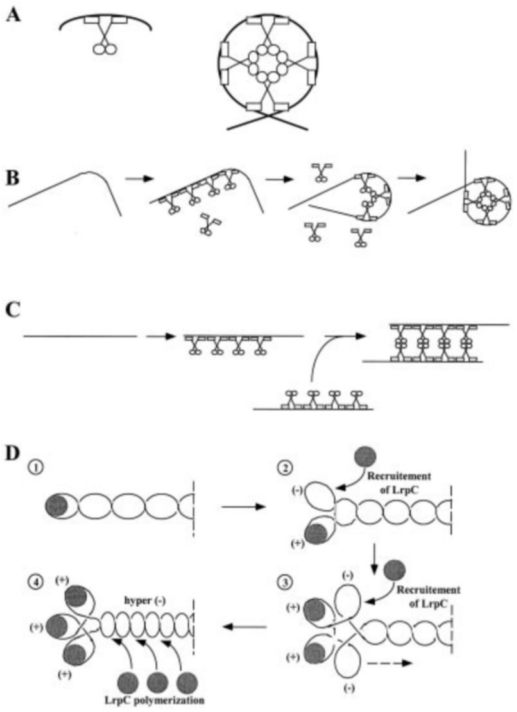

FIG. 8. **A model for LrpC-DNA interaction.** *A*, octameric model of quaternary structure of LrpC interacting with DNA adapted from comparison with the *P. furiosus* LrpA protein octameric model (25). N-terminal helix-turn-helix DNA-binding domain and C-terminal oligomerization domain are represented by *open squares* and *open circles*, respectively. *B*, interaction of LrpC with flexible/curved DNA induces a complete wrapping of the DNA around the protein to form a nucleosome-like structure. *C*, interaction of LrpC with straight DNA (*i.e.* uncurved or hyperconstrained) leads to polymerization of LrpC and bridging of DNA fragments through protein-protein interactions. *D*, interaction of LrpC with a negatively supercoiled plasmid DNA. LrpC creates a positively supercoiled loop that is compensated by a new negatively supercoiled loop. The latter is a target for LrpC. This model explains the formation of successive wrappings in a very close proximity by an invasive mechanism that induces partition of topological domains between LrpC-restrained positive supercoils and free negative ones.

DNA Topology and LrpC/DNA Interactions—We have shown that LrpC/DNA complex formation is influenced by DNA topology and, moreover, that LrpC constrains positive supercoiling. We propose that the formation of a first complex in supercoiled molecules is promoted by one curved region localized at one of the apices, as observed previously for the transcription activator NR1 (32) and the Tth 111 glutamine synthetase (33) (Fig. 7 and 8*D*, *1*). Because LrpC induces the formation of a positively supercoiled loop, a new negatively supercoiled loop is then

created in the vicinity of the first complex to maintain a constant linking number. The formation of a second complex is favored by cooperative effects, which promote LrpC recruitment to the flanking DNA regions (Fig. 8*D*, *2*). This will induce the formation of a new positive supercoil and subsequently of a compensatory negative supercoil that will be again targeted by an LrpC oligomer (Fig. 8*D*, *3*). This model explains the formation of successive wrappings in a very close proximity by an invasive mechanism, which induces partition of topological domains between LrpC-restrained positive supercoils and free negative ones (Fig. 8*D*, *4*). To our knowledge, we present the first visualization of such a partition in negative and positive supercoiled domains within a single DNA molecule and therefore demonstrate that positive supercoiling mediated by LrpC is caused by a right-handed DNA wrapping (Fig. 7, *b* and *c*). The presence of a right-handed DNA superhelix wrapped around a protein core in a negatively supercoiled environment represents a new topological paradox that could be explained by the following considerations.

The affinity of LrpC for DNA increases with supercoiling, either positive or negative, because supercoiling favors loop formation. Whatever their chirality, these loops promote protein/protein assembly, and the stabilization of the complexes leads to the formation of a right-handed DNA helix. Such DNA transition triggered by LrpC should require minimal energy, as shown for interaction of $(H3\text{-}H4)_2$ tetramer with supercoiled DNA (34).

Such a topological partition in the plasmid induces an accumulation of negative topological constraints in the free DNA, which reduces its flexibility. Consequently, right-handed DNA wrapping around the LrpC protein core is no longer favored, and an alternative mode of protein-protein interaction is adopted; any additional LrpC protein polymerizes along the hypernegatively supercoiled DNA (Figs. 7 and 8).

This bimodal assembly of LrpC within nucleoprotein complexes is related to two types of DNA condensation, determined by the topological state of DNA. The first one results from successive DNA wrappings mainly observed with linear fragments and in regions of negatively supercoiled DNA (Figs. 1, 2, and 7). The second one results from polymerization of LrpC along DNA and bridging of DNA segments within a circular plasmid to finally induce its folding. This could be observed with open circular plasmids (data not shown) or with slightly positive supercoiled plasmids, where right-handed DNA wrapping by LrpC led to a relaxation of the free DNA (Fig. 7), followed by additional polymerization of the protein along DNA. The same type of interactions (*i.e.* polymerization and bridging) is observed with "straight" uncurved DNA (data not shown; Fig. 8*C*).

LrpC, an Unusual DNA Architecture Protein—The capacities of LrpC to drastically modify DNA structure by DNA bending and wrapping, and the fact that it probably uses these properties to modulate the geometry of promoters, confirms that LrpC belongs to the DNA architectural protein family. However, it seems that LrpC possesses unusual properties among eubacterial DNA structuring proteins, including the Lrp-like family. Whereas *E. coli* Lrp has been proposed to wrap DNA (35), LrpC, along with the Smj12 protein from *Sulfolobus solfataricus* (which also overwinds DNA) and the PutR protein from *Agrobacterium tumefaciens*, are the only members of the Lrp-like family for which DNA wrapping has been firmly demonstrated (36, 37). Looped structures formed by LrpC where 80 bp of DNA is wrapped resemble eukaryotic dimers of $(H_3\text{-}H_4)$ and archaeal HMf or HTz tetrasomes (Fig. 2; 38, 39). Eukaryotic dimers of $(H_3\text{-}H_4)$ (35) and HMf tetramers (40) are able, under certain conditions, to constrain positive supercoils, as observed for LrpC. Other proteins that activate transcription, such as the eukaryotic transcription factors UBF or SWI/SNF or the *B. subtilis* PurR regulator, are known to bind upstream of the promoters they regulate and to introduce one positive supercoil (41–44). Therefore, it is likely that the capacity of LrpC to induce right-handed supercoiling is involved in its regulatory activity. In addition, like the HMf proteins, eukaryotic histones and the high mobility group proteins, LrpC highly compacts DNA. Such ability has not been described thus far for other members of the Lrp-like family. This work shows that the *B. subtilis* LrpC protein displays a mosaic of properties present in archaeal and eukaryotic histones, Lrp-like proteins, transcription factors, and eubacterial DNA-structuring proteins. Consequently, LrpC is a unique member of the DNA architectural family of proteins.

A fascinating hypothesis is that micro-organisms have developed a DNA overwinding activity to compensate for the DNA underwinding activity displayed by more common nucleoid-associated proteins such as H-NS, HU, IHF, or Fis. The LrpC protein could be a prototypical member of a new family of proteins that overwinds DNA and, together with topoisomerases, modulates the global supercoiling density or, more likely, the local DNA topology during certain DNA transactions. Indeed, at 10 to 80 tetramers per cell, LrpC is not particularly abundant in the cell under normal growth conditions (16); this could limit its role as global chromosome organizer and suggests a role in sensing locally DNA architecture. In light of what we have learned concerning LrpC, it would be interesting to evaluate the DNA binding and DNA structuring properties of the six other *B. subtilis* Lrp/AsnC proteins to gain a fuller appreciation of the role for this family in bacterial physiology.

Acknowledgments—We thank R. Exley for help with the English language, P. Deighan, F. Confalonieri, and W. F. Stevens for helpful discussions, and S. Lyonnais for help with figures.

REFERENCES

1. Azam, T. A., and Ishihama, A. (1999) *J. Biol. Chem.* **274,** 33105–33113
2. Alonso, J. C., Gutierrez, C., and Rojo, F. (1995) *Mol. Microbiol.* **18,** 471–478
3. Goosen, N., and van de Putte, P. (1995) *Mol. Microbiol.* **16,** 1–7
4. Perez-Martin, J., and de Lorenzo, V. (1997) *Annu. Rev. Microbiol.* **51,** 593–628
5. Flashner, Y., and Gralla, J. D. (1988) *Cell* **54,** 713–721
6. Preobrajenskaya, O., Boullard, A., Boubrik, F., Schnarr, M., and Rouvière-Yaniv, J. (1994) *Mol. Microbiol.* **13,** 459–467
7. Aki, T., and Adhya, S. (1997) *EMBO J.* **16,** 3666–3674
8. Werner, M. H., Huth, J. R., Gronenborn, A. M., and Clore, G. M. (1995) *Cell* **81,** 705–714
9. Bianchi, M. E. (1994) *Mol. Microbiol.* **14,** 1–5
10. Reeves, R., Leonard, W. J., and Nissen, M. S. (2000) *Mol. Cell. Biol.* **20** 4666–4679
11. Beloin, C., Ayora, S., Exley, R., Hirschbein, L., Ogasawara, N., Kasahara, Y., Alonso, J. C., and Le Hégarat, F. (1997) *Mol. Gen. Genet.* **256,** 63–71
12. Belitsky, B. R., Gustafsson, M. C., Sonenshein, A. L., and Von Wachenfeldt, C. (1997) *J. Bacteriol.* **179,** 5448–5457
13. Dartois, V., Liu, J., and Hoch, J. A. (1997) *Mol. Microbiol.* **25,** 39–51
14. Kunst, F., Ogasawara, N., Moszer, I., Albertini, A. M., Alloni, G., Azevedo, V., Bertero, M. G., Bessieres, P., Bolotin, A., Borchert, S., Borriss, R., Boursier, L., Brans, A., Braun, M., Brignell, S. C., Bron, S., Brouillet, S., Bruschi, C. V., Caldwell, B., Capuano, V., Carter, N. M., Choi, S. K., Codani, J. J., Connerton, I. F., Danchin, A., and et al. (1997) *Nature* **390,** 249–256
15. Brennan, R. G., and Matthews, B. W. (1989) *J. Biol. Chem.* **264,** 1903–1906
16. Beloin, C., Exley, R., Mahe, A. L., Zouine, M., Cubasch, S., and Le Hégarat, F. (2000) *J. Bacteriol.* **182,** 4414–4424
17. Muzard, G., Theveny, B., and Révet, B. (1990) *EMBO J.* **9,** 1289–1298
18. Larquet, E., Furrer, P., Stasiak, A., Dubochet, J., and Révet, B. (1995) *J. Biomol. Struct. Dyn.* **12,** 134
19. Tapias, A., Lopez, G., and Ayora, S. (2000) *Nucleic Acids Res.* **28,** 552–559
20. Le Cam, E., and Delain, E. (1995) in *Visualization of Nucleic Acids* (Morel, G., ed), pp. 333–358, CRC Press, Boca Raton, FL
21. Dubochet, J., Ducommun, N., Zollinger, M., and Kellenberger, E. (1971) *J. Ultrastruct. Res.* **35,** 147–167
22. Joanicot, M., and Révet, B. (1987) *Biopolymers* **26,** 315–326
23. Delain, E., Fourcade, A., Poulin, J. C., Barbin, A., Coulaud, D., Le Cam, E., and Paris, E. (1992) *Microsc. Microanal. Microstruct.* **3,** 457–470
24. Delain, E., and Le Cam, E. (1995) in *Visualization of Nucleic Acids* (Morel, G., ed), pp. 35–56, CRC Press, Boca Raton, FL
25. Leonard, P. M., Smits, S. H., Sedelnikova, S. E., Brinkman, A. B., de Vos, W. M., van der Oost, J., Rice, D. W., and Rafferty, J. B. (2001) *EMBO J.* **20,** 990–997
26. Grove, A., Galeone, A., Mayol, L., and Geiduschek, E. P. (1996) *J. Mol. Biol.*

260, 120–125
27. Trifonov, E. N. (1991) *Trends Biochem. Sci* **16,** 467–470
28. Travers, A., and Klug, A. (1987) *Nature* **327,** 280–281
29. Nadeau, J. G., and Crothers, D. M. (1989) *Proc. Natl. Acad. Sci. U. S. A.* **86,** 2622–2626
30. Bolshoy, A., McNamara, P., Harrington, R. E., and Trifonov, E. N. (1991) *Proc. Natl. Acad. Sci. U. S. A.* **88,** 2312–2316
31. Haran, T. E., Kahn, J. D., and Crothers, D. M. (1994) *J. Mol. Biol.* **244,** 135–143
32. Révet, B., Brahms, S., and Brahms, G. (1995) *Proc. Natl. Acad. Sci. U. S. A.* **92,** 7535–7539
33. Mary, J., and Révet, B. (1999) *J. Mol. Biol.* **286,** 121–134
34. Hamiche, A., Carot, V., Alilat, M., De Lucia, F., O'Donohue, M. F., Révet, B., and Prunell, A. (1996) *Proc. Natl. Acad. Sci. U. S. A.* **93,** 7588–7593
35. Wang, Q., and Calvo, J. M. (1993) *EMBO J.* **12,** 2495–2501
36. Jafri, S., Evoy, S., Cho, K., Craighead, H. G., and Winans, S. C. (1999) *J. Mol. Biol.* **288,** 811–824
37. Napoli, A., Kvaratskelia, M., White, M. F., Rossi, M., and Ciaramella, M. (2001) *J. Biol. Chem.* **276,** 10745–10752
38. Dong, F., and van Holde, K. E. (1991) *Proc. Natl. Acad. Sci. U. S. A.* **88,** 10596–10600
39. Musgrave, D. R., Sandman, K. M., and Reeve, J. N. (1991) *Proc. Natl. Acad. Sci. U. S. A.* **88,** 10397–10401
40. Musgrave, D., Forterre, P., and Slesarev, A. (2000) *Mol. Microbiol.* **35,** 341–349
41. Putnam, C. D., Copenhaver, G. P., Denton, M. L., and Pikaard, C. S. (1994) *Mol. Cell. Biol.* **14,** 6476–6488
42. Quinn, J., Fyrberg, A. M., Ganster, R. W., Schmidt, M. C., and Peterson, C. L. (1996) *Nature* **379,** 844–847
43. Shin, B. S., Stein, A., and Zalkin, H. (1997) *J. Bacteriol.* **179,** 7394–7402
44. Ozoline, O. N., Deev, A. A., and Trifonov, E. N. (1999) *J. Biomol. Struct. Dyn.* **16,** 825–831
45. Koo, H. S., and Crothers, D. M. (1988) *Proc. Natl. Acad. Sci. U. S. A.* **85,** 1763–1767
46. de Santis, P., Palleschi, A., Savino, M., and Scipioni, A. (1990) *Biochemistry* **29,** 9269–9273